The International Journal of Nautical Archaeology (2007) **36**.1: 167–176
doi: 10.1111/j.1095-9270.2006.00131.x

Impacts of Alexandria's Heptastadion on coastal hydro-sedimentary dynamics during the Hellenistic period: a numerical modelling approach

Bertrand Millet

Centre d'Océanologie de Marseille, UMR CNRS—Université de la Méditerranée 6535, Campus de Luminy, case 901, 13288 Marseille Cedex 9, France

Jean-Philippe Goiran

Archéorient, UMR CNRS 5133, Maison de l'Orient et de la Méditerranée, 7 rue Raulin, 69007 Lyon, France

After its foundation in 331 BC, Alexandria was linked to the island of Pharos by the Heptastadion. The present study aims at understanding the impact of this building on the local water and sand dynamics. We used numerical models to compute the wind-induced currents and sediment re-suspension, comparatively without and in the presence of the Heptastadion. Results suggest that the Heptastadion was not only a link structure to reach the Pharos island, but a structure liable to reduce the sandy sediment dynamics in the eastern harbour, and then to protect the eastern harbour from infilling by the allochthonous sand drift.

Key words: modelling, palaeodynamics, sedimentology, Heptastadion, Alexandria, Egypt.

In 331 BC Alexander the Great decided to build the first city bearing his name, to the west of the Nile delta, behind an island named Pharos by the Greeks (Homer, in Garvie, 1994). The configuration of the site made possible the creation of two harbours on either side of the causeway, linking the city to Pharos (Fig. 1). The Heptastadion, as this causeway became to be known (Strabo, in Bernand, 1998; Empereur, 1998) was seven *stadia* long (*c*.1240 m if one stadium is taken to be 177 m) (Yoyotte *et al.*, 1997). 'The embankment [the Heptastadion] forms a bridge extending from the mainland to the western portion of the island [of Pharos)] ... However, this work formed not only a bridge to the island but also an aqueduct, at least when Pharos was inhabited (Strabo, *Geography* 17.I.6, in Jones, 1959). A year earlier, in 332 BC, Alexander achieved a similar technical feat in Tyre. Over a six-month span, his engineers managed to link the island of Tyre to the Phoenician coast with a causeway, a distance of *c*.600 m.

Alexandria's Heptastadion was constructed by Deinocrates, who also drew up the architectural plans for the city. It seems that the causeway was built in the north-south extension of the street network (Hesse *et al.*, 2002), which had a milesian orthogonal organisation (Etienne *et al.*, 2000), studied and published by El Falaki (1872). In this way, from the end of the 4th century BC, the Heptastadion separated the eastern harbour and the western harbour, but following the description given by Strabo (Jones, 1959: 27), the Heptastadion had two narrow gates, respectively located at the northern and southern extremities, in order to allow the navigation of boats between the two harbours. Unfortunately, Strabo gave no information about the dimensions of these two gates, and we chose to consider in our study two openings each 25 m long and 2 m deep, representing a cumulative open-water section of 100 m^2 and 6% of the whole Heptastadion water section considered in the model, which is 1666 m^2. Despite the presence of these narrow connections, the

Published by Blackwell Publishing Ltd. 9600 Garsington Road, Oxford OX4 2DQ, UK and 350 Main Street, Malden, MA 02148, USA.

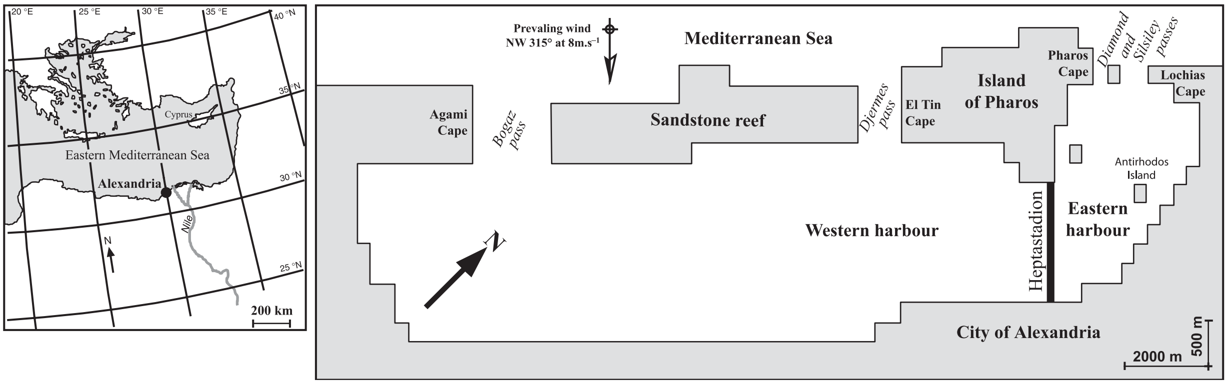

Figure 1. General map of the studied area and (right) representation of the city of Alexandria and surrounding coastal zones during the Hellenistic period (4th to 1st centuries BC).

Heptastadion is assumed to induce drastic changes in the palaeogeographical configuration of the two harbours, with significant disturbances in water and sediment dynamics.

Indeed, the series of small harbours constructed around the rim of the basin confirms that ancient societies must have modified the environment in order to act effectively against the influence of currents, and the infilling of those areas. The present study was focused on the role played by the Heptastadion in the modification of the coastal currents and sediment-transport, and especially on its eventual contribution to prevent the eastern harbour from rapid sediment-infilling. Two numerical models were used, firstly to compute the wind-induced currents and waves, and secondly the sediment re-suspension rates, comparing these before and after the building of the Heptastadion. First, the models had to be adapted to the surviving eastern harbour, in order to calibrate the numerical parameters from the recent field measurements available on this site (Lotfy and Badr, 1999). Second, the models were applied to the whole coastal domain (both eastern and western harbours) in antiquity, and results allowed us to emphasize major hypotheses concerning the Heptastadion's impact on the water and sediment coastal dynamics.

Material and methods

Bathymetric maps of the coastal region of Alexandria were available from the French Service Hydrographique et Océanographique de la Marine (SHOM, 1990), from the United Kingdom Hydrographic Office (UKHO, 1989) and from the Hydrographic Office of the Admiralty (Smyth *et al.*, 1833). We have adapted a palaeobathymetric map to the end of the Classical Greek period (Fig. 1), using the available bathymetric data, and taking into account historical bathymetric data obtained by coring. This map was defined in considering the following main parameters: the age and depth of the facies obtained by coring in the western and eastern harbours and in the tombolo area; and the estimated subsidence of 5 m to be considered since antiquity (El Falaki, 1872; Goddio *et al.*, 1998; Goiran *et al.*, 2003). In addition, Fig. 1 presents the location of the Heptastadion, as it was taken into account in the second set of computations to quantify the impact of this structure on the water and sediment dynamics.

The nature of the coastal configuration means that the dominant local wind hits the coastal ridge at a perpendicular angle. We considered into the numerical models the north-westerly dominant wind (NW–315°) with the constant velocity of 8 $m.s^{-1}$, according to the meteorological stations of Alexandria, and confirmed by local scientists in a recent study (Lotfy and Badr, 1999). Indeed, it appears that the orientation of the dominant winds has not changed since antiquity, as indicated by numerous authors of the Graeco-Roman period, such as Strabo (1st century BC) who wrote that the streets of the city were oriented so as to be cooled by the summer sea-breeze during the hot period.

The numerical model considered to compute the wind-driven currents was a classical 2D horizontal model using depth-integrated equations of the fluid dynamics, and which was previously used and described in different coastal areas (Millet, 1989; Millet *et al.*, 2000). The model computes depth-averaged current velocities within the homogeneous water body under a constant wind force. This system is solved by a classical semi-implicit Alternating Direction Implicit (ADI) scheme and current-fields are considered after 48 hours of simulation in order to reach the steady state of the numerical computations. The model was first applied to the eastern harbour at the present time by using a 43 × 59 grid of regular 41.66 m squared meshes and a time-step of 2 s, and then adapted this to both harbours in antiquity by using a 19 × 70 grid of regular 208.33 m squared meshes and a time step of 10 s.

The formulations considered to compute the height and the period of the wind-induced waves are proposed by the CERC (1975) as follows:

$$g.H/W^2 = 0.283 \cdot \mathrm{th}[0.53 \cdot (g.h/W^2)^{0.75}] \cdot \mathrm{th}[(0.0125 \cdot (g.F/W^2)^{0.42})/(\mathrm{th}(0.53 \cdot (g.h/W^2)^{0.75}))] \quad (1)$$

$$g.T/(2 \cdot \pi \cdot W) = 1.2 \cdot \mathrm{th}[0.833 \cdot (g.h/W^2)^{0.375}] \cdot \mathrm{th}[(0.077 \cdot (g.F/W^2)^{0.25})/(\mathrm{th}(0.833 \cdot (g.h/W^2)^{0.375}))] \quad (2)$$

where: (H) the wave height; (T) the wave period; (g) the gravity; (h) the depth of the waterbody; (F) the fetch and (W) the wind speed.

The formulations considered to compute the bottom-stresses induced by the combined effect of both wind-induced currents and waves, and the re-suspension rates of the non-cohesive sandy sediment of the Alexandria harbours, were taken from the practical algorithms proposed by Soulsby (1997), which are well adapted to marine sediments in coastal environments. The bottom-stress (τ_C) only induced by wind-induced currents is expressed as:

$$\tau_C = \rho \cdot C_d \cdot U^2 \quad (3)$$

The time-averaged bottom-stress (τ_w) only induced by wind-induced waves is:

$$\tau_w = 1/2 \cdot (\rho \cdot f_w \cdot U_w^2) \quad (4)$$

where: (U) the depth-averaged current-velocity, which was previously computed by the current model; (ρ) the water-density; (C_d) the drag-coefficient; (f_w) the wave-friction factor and (U_w) the near-bed orbital velocity amplitude, which is expressed as:

$$U_w = (\pi \cdot H/T) \cdot (1/\sinh[4 \cdot \pi^2 \cdot H/(g.T^2)]) \quad (5)$$

The wave-friction factor (f_w) adapted to rough turbulent flow is expressed as follows, still according to Soulsby (1997):

$$f_w = 1.39 \cdot (A/z_o)^{-0.52} \quad (6)$$

where: (z_o) the bed roughness length and (A) the near-bed orbital excursion, expressed as:

$$A = U_w \cdot T/(2\pi) \quad (7)$$

The resulting bottom-stress (τ_R) due to the combined effects of both currents and waves is expressed as:

$$\tau_R = \tau_C \cdot (1 + 1.2 \cdot [\tau_w/(\tau_w + \tau_C)]^{3.2}) \quad (8)$$

The threshold bed shear-stress (τ_{cr}) for sediment re-suspension ($N.m^{-2}$) is expressed from the Shields threshold parameter (θ_{cr}), following the approach confirmed by Soulsby and Whitehouse (1997) and cited in Soulsby (1997):

$$\tau_{cr} = \theta_{cr} \cdot g \cdot (\rho_s - \rho) \cdot d \quad (9)$$

where: (θ_{cr}) the Shields threshold parameter; (ρ_s) the grain density; (d) the grain diameter.

The Shields threshold parameter θ_{cr} is defined as:

$$\theta_{cr} = [0.3/(1 + 1.2 \cdot D^*)] + 0.055 \cdot [1 - e^{(-0.02 \cdot D^*)}]$$

with D^*, the dimensionless grain size is given by:

$$D^* = d \cdot (g \cdot [(\rho_s/\rho) - 1] / \nu^2)^{1/3}$$

where: (ν) the kinematic viscosity of fresh water considered at temperature 20 °C ($\nu = 10^{-6} m^2.s^{-1}$).

Finally, the rate of sediment re-suspension (R), by surface units, under the combined effect of currents and waves is:

$$R = C_M \cdot [1 - (\tau_{cr}/\tau_R)] \quad (10)$$

($R > 0$) where: (C_M) the maximal rate of re-suspension ($kg.m^{-2}.s^{-1}$)

Results

Validation of the current model in the present eastern harbour

The current model was first adapted to the present eastern harbour, considering the SHOM bathymetric map and the constant force of the dominant NW–315° (8 $m.s^{-1}$) wind regime. Figure 2 presents the computed current field within the eastern harbour, with depth-averaged velocities, which are also considered at steady state corresponding to the wind force. The bathymetry considered in the model ranges from 1 m near the shore to 12 m at the vicinity of the inlets, with a spatial averaged value of 4.5 m over the whole domain. The computed velocities range from the minimum of 0.01 $m.s^{-1}$ in the middle of the gyratory currents to the maximum of 0.28 $m.s^{-1}$ through the passes, with a spatial averaged value of 0.086 $m.s^{-1}$.

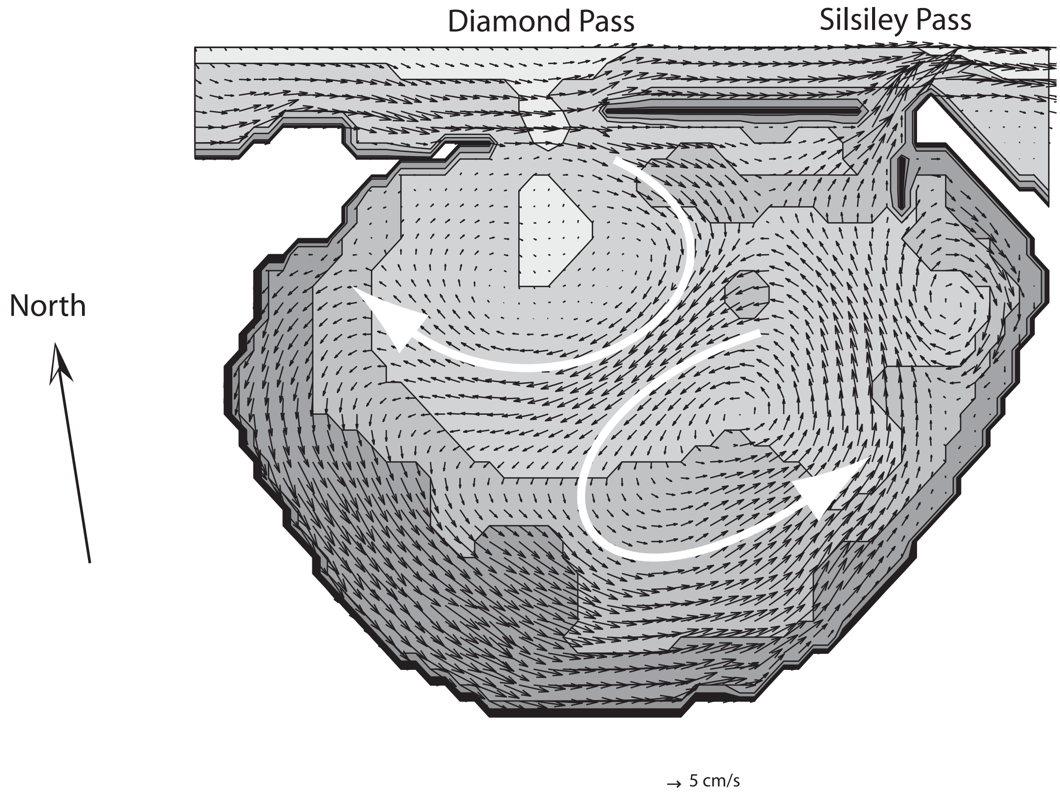

Figure 2. Current-fields in the eastern harbour of Alexandria today, computed by the 2D numerical model with a constant NW–315° (8 m.s^{-1}) wind, with the bathymetric range considered in the model; highlighted arrows represent field-measurements from Lotfy and Badr (1999).

This pattern can be compared with the current measurements which have been performed in the eastern harbour by the Coastal Research Institute of Alexandria (Lotfy and Badr, 1999). Though the current measurements published by these authors represents a synthetic interpretation of field data locally recorded at some stations both at the surface and near the bottom along short periods of immersion, it is possible to notice relatively good agreements between interpolated measurements and computed current-structures, especially considering the clockwise north-western and anticlockwise south-eastern gyres that are highlighted in Fig. 2. It is also noteworthy that both experiments and modelling confirm the dominant eastward water-circulation through the eastern harbour, from an inflow located through the eastern Diamond pass to an outflow located through the El Silsiley pass (Figs 1 and 2). Moreover, computed velocities are in good agreement with current measurements that ranged between 0.03 and 0.70 m.s^{-1} following Lotfy and Badr, keeping in mind that observations are not depth-averaged values but local recordings at specific depths (near-bottom and water-surface).

Calibration of the sediment-dynamics model in the present eastern harbour

The sand-dynamics model was then performed in the present eastern harbour, considering the results of the current model previously described, the computation of the waves induced by the same dominant NW–315° (8 m.s^{-1}) wind regime, and the field measurements of the sand-dynamics performed in the eastern harbour of Alexandria for the whole 1936–1986 period and published by Lotfy and Badr (1999). The wave-heights and -periods are computed according to equations (1) and (2). The maximum values range from H = 0.90 m (T = 4.0 s) in the western harbour at the vicinity of the passes, and H = 0.62 m (T = 3.2 s) within the harbour in nearshore areas aligned with the passes following the wind direction. The minimum values are H = 0.10 m (T = 1.2 s) within the harbour in all the other peripheral nearshore areas. These results are in good agreement with measurements and within the range of the observed variability published by Lotfy and Badr for maximum wave heights (H = 0.75–1.23 m) and maximum wave period (T = 4–11 s).

Concerning the sediment, Lotfy and Badr (1999) confirm the silicate and sandy nature of the sediment in the harbour today, with grain diameters (*d*) ranged from 0.063 mm to 2 mm and a grain-density ρ_s = 2650 kg.m^{-3}. Moreover, Lotfy and Badr emphasize the mean annual re-suspension rate of 13.38 · 10^3 m^3.year^{-1} of sands in the whole eastern harbour and over the 50-year period 1936–86, making a local sediment flux of 0.416 · 10^{-6} kg.m^{-2}.s^{-1} and a cumulated re-suspension rate of 1.12 kg.s^{-1} in the present eastern harbour. According to these published measurements, we adapted the empirical algorithms proposed by Soulsby (1997) allowing the computation of the wind- and wave-induced bottom stresses and the threshold bed shear-stress for marine sands, previously presented through the equations (1) to (9).

We considered in our computations the finest fraction of the observed non-cohesive sandy sediment with a grain diameter d = 0.063 mm. Moreover, we chose a bed-roughness length z_o = 2 mm and a drag-coefficient C_d = 3.47 · 10^{-3}, following Soulsby 1997 that corresponds to a rough unrippled sand-bed with water-depths ranged between 2 and 20 m. We obtained a threshold bed shear-stress τ_{cr} = 10.6 · 10^{-2} N.m^{-2} according to the equation (9) that represents the minimum threshold value according to the finest fraction of the local sandy sediment. Then we calibrated the equation (10) to quantify the right value of the maximal rate of re-suspension (C_M) corresponding to the empirical re-suspension rate of 1.12 kg.s^{-1}, and we obtained the calibrated value of C_M = 1.103.10^{-5} kg.m^{-2}.s^{-1}.

Water circulation in the harbours in antiquity: the Heptastadion impact

The current model, first validated in the present eastern harbour, was then adapted to both harbours in antiquity, considering the adapted palaeobathymetric map previously described (Fig. 1) and again the constant force of the dominant NW–315° (8 m.s^{-1}) wind regime. The bathymetry considered in the model within the western harbour ranges from 1 m nearshore to 5 m at the vicinity of the passes with the averaged value of 3 m, and respectively ranges within the eastern harbour from 1 m to 10 m with the averaged value of 4.74 m. Figure 3 presents the computed depth-averaged current velocities and the spatial hydrodynamic structure in both harbours in antiquity, considered at the steady state of the most frequent wind-regime, without (Fig. 3a) and in the presence (Fig. 3b) of the Heptastadion.

Modelling results without the Heptastadion (Fig. 3a) emphasize a dominant eastward circulation pattern, flowing from an inflow located through the main Bogaz pass (section 1) of the western harbour toward the eastern harbour, through the famous site of the tombolo (section 2) south of Pharos island. In the western harbour, a secondary outflow is also located through Djermes pass (section 3) west of Pharos island. In the eastern harbour, an inflow is effective through north-western Diamond pass (section 4) as the main outflow of the whole system is located through north-eastern Silsiley pass (section 5), that features to the eastern harbour in antiquity a circulation-pattern quite similar to present time. The computed velocities range from the minimum of 0.02 m.s^{-1} in the middle of the gyres to the maximum of 0.30 m.s^{-1} through the passes, with spatial averaged values of 0.076 m.s^{-1} and 0.10 m.s^{-1} respectively within the western and eastern harbours.

Modelling results in the presence of the Heptastadion (Fig. 3b) emphasize a reinforced water-flux through Djermes pass (section 3) to equilibrate the water-budget within the western harbour, and a weaker circulation within the eastern harbour, separated by the Heptastadion from any flux flowing from the western harbour. The circulation-pattern within the eastern harbour remains featured by an eastward transit of water from a western inflow through Diamond pass (section 4) to an eastern outflow through Silsiley pass (section 5), but it is possible to notice the increasing clockwise gyre in the eastern part of the harbour, as is the case in the same site at present time. The computed velocities range from the minimum of 0.02 m.s^{-1} in the middle of the gyres to the maximum of 0.30 m.s^{-1} through the passes, with spatial averaged values of 0.072 m.s^{-1} and 0.07 m.s^{-1} respectively within the western and eastern harbours. The computed velocities through the two narrow gates of the Heptastadion were 0.16 m.s^{-1} and 0.14 m.s^{-1}, respectively for the northern and the southern extremities. Table 1 presents the computed water fluxes though the 5 sections previously defined, comparatively without and in the presence of the Heptastadion.

Sediment-fluxes in the harbours in antiquity: the Heptastadion impact

The sand dynamics model, first calibrated in the present eastern harbour, was then adapted to both harbours in antiquity, considering the adapted palaeobathymetric map previously described (Fig. 1) and the computation of the waves

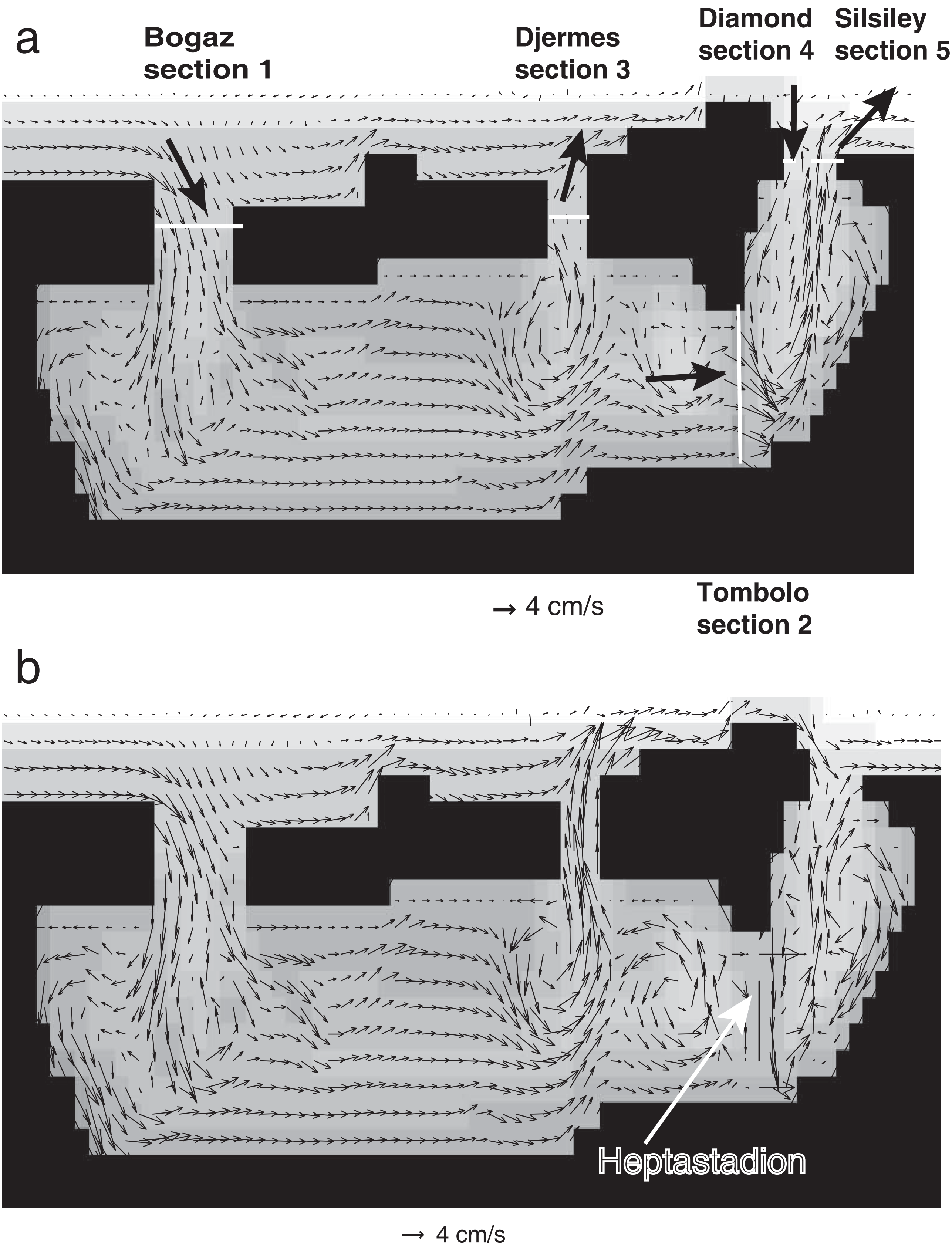

Figure 3. Current-fields in the Alexandria harbours in antiquity computed by the 2D numerical model with a constant NW–315° (8 m.s^{-1}) wind, respectively (a) without and (b) with the Heptastadion.

Table 1. *Computed water fluxes ($m^3.s^{-1}$) through 5 sections defined in both western and eastern harbours in Antiquity, comparatively without and in the presence of the Heptastadion*

Computed Water Fluxes ($m^3.s^{-1}$)	Section 1 *Bogaz pass inflow*	Section 2 *Tombolo eastward*	Section 3 *Djermes pass outflow*	Section 4 *Diamond pass inflow*	Section 5 *Silsiley pass outflow*
No Heptastadion	371	306	65	165	471
With Heptastadion	332	15	317	130	145

Table 2. *Results of the sand dynamics model adapted to the harbours in Antiquity, and compared without and in the presence of the Heptastadion*

	Western Harbour		Eastern Harbour	
	No Heptast.	*With Heptast.*	*No Heptast.*	*With Heptast.*
Spatial averaged Current Velocity ($m.s^{-1}$)	0.076	0.072	0.10	0.073
Spatial averaged Bottom Stress ($*10^{-2}$ $N.m^{-2}$)	2.93	2.67	5.27	2.64
Spatial Averaged Resuspension Rate ($*10^{-6}$ $kg.m^{-2}.s^{-1}$)	0.05	0.071	0.48	0.007
Cumulated Resuspension Rate ($kg.s^{-1}$)	1.07	1.50	1.83	0.028

induced by the same dominant NW–315° (8 $m.s^{-1}$) wind-regime. We considered again the finest fraction of the sandy sediment with a grain diameter d = 0.063 mm, and the same set of coefficients as previously calibrated in the eastern harbour at the present.

The waves computations (height and period) according to the equations (1) and (2) present the same results with and without the presence of the Heptastadion. The maximum values range from H = 0.74 m (T = 3.6 s) in the western harbour, or H = 0.95 m (T = 4.1 s) in the eastern harbour, at the vicinity of the passes, and H = 0.40 m (T = 2.9 s) within the both harbours in nearshore areas aligned with the passes following the wind-direction. The minimum values are H = 0.17 m (T = 1.5 s) in the western harbour, and H = 0.11 m (T = 1.2 s) in the eastern harbour, in all the other peripheral nearshore areas.

Modelling results computed with and without the presence of the Heptastadion are presented in Table 2 and expressed as: (i) the depth-averaged current velocity spatially averaged within each harbour ($m.s^{-1}$); (ii) the wind- and wave-induced resulting bottom stress averaged within each harbour (10^{-2} $N.m^{-2}$); (iii) the re-suspension rate of sediment averaged within each harbour (10^{-6} $kg.m^{-2}.s^{-1}$) and (iv) the cumulated re-suspension rate of sediment integrated over the whole area of each harbour ($kg.s^{-1}$).

Comparative results from the sand-dynamics model with and without the presence of the Heptastadion (Table 2) confirm a drastic impact of this structure on the sediment erosion in the eastern harbour, and a weaker incidence in the western harbour. Indeed, results show that the presence of the Heptastadion induces: a bottom shear-stress (current and waves) decreasing of 50% and 9% respectively in the eastern and western harbour; and a cumulated re-suspension rate decreasing of 98% in the eastern harbour but increasing of 40% in the western harbour.

Discussion and conclusion

Numerical models transposition from the present time to antiquity

The current model adapted to Alexandria's present eastern harbour gives good results compared to field observations locally available (Fig. 2), despite the fact that measurements were performed on two levels only (near the surface and near the bottom), as computed velocities were averaged on the whole water-column. These results encouraged the transposition of the current model on a new grid corresponding to the bathymetry and morphology of the harbours in antiquity. This transposition was reinforced by the knowledge, recently published by Franck Goddio (Goddio *et al.*, 1998), about the design of the peripheral structures within the eastern harbour in antiquity (Fig. 1), which have been taken into account in the numerical grid of our model. Therefore, we had to hypothesize that the nature of the sandy sediment remained approximately the same from antiquity to the present, in order to confirm the model representativity of the local processes in antiquity. The bathymetry relating to antiquity was evaluated from several borehole campaigns which allowed to reconstitute the water-column and the sea-bottom granulometry. It is noteworthy that the sedimentological data obtained from the recent borehole campaigns confirmed the persistence of sand fractions from the 4th millennium BC (Goiran *et al.*, 2003) until the present day (Frihy *et al.*, 1996), within both the eastern and western harbours.

Thus, the sand dynamics model adapted to the present eastern harbour, allowed us to quantify a calibrated value for the maximum re-suspension rate of sediment (C_M) that represents a drastic coefficient controlling the formulation of the wind- and wave-induced re-suspension rate of sediment. Anyway, we chose to develop all the computations with the finest fraction of the sands ($d = 0.063$ mm), to get the maximum values of re-suspension rates and prevent our comparative study of the Heptastadion impact from any underestimation that could have occurred in considering coarser fractions. In addition, following the comments of Strabo (Jones, 1959: 31), we confirm that the transposition of the same climatic context, and especially the same wind regime, in Mediterranean regions along the last 2300 years remains a relevant hypothesis.

Therefore it is interesting to compare the model results respectively computed in the eastern harbour today and in antiquity, in the presence of the Heptastadion, in order to discuss the drastic decreasing of the re-suspension rate from 1.12 (at present) to 0.028 $kg.s^{-1}$ (in antiquity). Actually, the bathymetry considered in the model is similar today and in antiquity (mean depth 4.5 and 4.74 m respectively) and current velocities are slightly higher at the present time than in antiquity (mean velocity 0.086 and 0.073 $m.s^{-1}$ respectively). Thus the lower rate for sandy sediment re-suspension computed in antiquity in the eastern harbour can be only related to the weaker wave-heights and -periods (maxi H = 0.40 m and maxi T = 2.9 s) compared to today (maxi H = 0.62 m and maxi T = 3.2 s). This difference in wave-dynamics, weaker in antiquity than at present, might be induced by the very complex morphology of the eastern harbour, more confined from offshore connections in antiquity than at present time, due to the narrow passes, islands and other built structures described by Goddio *et al.* (1998) and taken into account in current and sediment models.

The Heptastadion impact on the coastal water and sediment dynamics

Model results show that the construction of the Heptastadion led to important modifications in the current and sediment dynamics, especially within the eastern harbour. First, considering the western harbour, the comparison between Figs 3a and 3b confirms the drastic reinforcement of the circulation through the Djermes pass (section 3) with water-outflow increasing from 65 to 332 $m^3.s^{-1}$ (Table 1). On the contrary, the main circulation patterns within the harbour do not seem affected by the presence of the Heptastadion, with similar values of averaged current-velocities without (0.076 $m.s^{-1}$) and in the presence of the Heptastadion (0.072 $m.s^{-1}$). More generally, and considering sediment aspects, the modelling results confirm that the whole western harbour can be considered as a coastal zone featured by active erosion processes, both with and without the Heptastadion, with a high level of bottom-stress (2.93 and 2.67 $N.m^{-2}$ respectively) and high cumulated re-suspension rates (1.07 and 1.50 $kg.s^{-1}$ respectively). This increasing of 40% of the cumulated re-suspension rates (Table 2), induced by the presence of the Heptastadion, can be attributed to the increasing circulation patterns at the vicinity of the Djermes pass. It is noteworthy to consider that active erosion processes still characterize the western harbour, where most of Ottoman structures have now disappeared. Thus, it is possible to consider that the western harbour might have functioned, in antiquity and before the construction of the Heptastadion, as a major source of eroded sediment available for the eastern harbour, flowing eastward through the tombolo site (section 2) with the water flux of 306 $m^3.s^{-1}$.

Second, considering the eastern harbour, the comparison between Figs 3a and 3b and results in Table 1 confirm the drastic decreasing of the water-circulation after the construction of the Heptastadion, both through the western Silsiley pass (section 5) where fluxes decrease from 471 to 145 $m^3.s^{-1}$, and within the harbour where the strong north-eastward transit of water and sediment had disappeared. Actually, results in Table 2 confirm the decreasing of the averaged current velocities from about 0.10 to 0.073 $m.s^{-1}$ and the drastic decreasing of the bottom-stress of about 50%, from the exceptional value of 5.27 $N.m^{-2}$ to the lower value of 2.64 $N.m^{-2}$ that is a value quite similar to those featuring the western harbour. Moreover, this strong decreasing of the water-dynamics within the eastern harbour leads to the disappearing of the sandy sediment re-suspension (d = 0.063 mm), with the drastic decreasing of the cumulated re-suspension rate from 1.83 $kg.s^{-1}$ to the very low value of 0.028 $kg.s^{-1}$ (Table 2). Inversely, we have seen that the wave-heights and -periods are not influenced by the construction of the Heptastadion (maxi H = 0.40 m/T = 2.9 s; mini H = 0.11 m/T = 1.2 s in nearshore areas) that is the consequence of the cross-shore direction of the wind-induced wave-propagation (SE–135°), which is aligned parallel to the Heptastadion. Thus, the drastic decreasing of the sandy sediment dynamics in the eastern harbour in the presence of the Heptastadion is essentially due to the reduced current-velocities associated with the removal of the north-eastward flux through the harbour.

Finally, it is possible to consider that the eastern harbour might have functioned, in antiquity and after the construction of the Heptastadion, as a basin featured by a sediment budget relatively equilibrated in considering: no more inflow of sand particles from the western harbour; no infilling by offshore particles by considering a mass balance between the presumed sediment import through Diamond pass and export through Silsiley pass; thirdly, *in-situ* re-suspension processes limited to the fine fractions of silts and clays (d < 0.063 mm) and liable locally to induce a high level of turbidity; and lastly a notable export of these fine particles through the Silsiley pass (section 5) with the water outflow of 145 $m^3.s^{-1}$.

The results reinforce the idea of a desire to protect the eastern harbour against a rapid infilling of sandy sediment

Our modelling approach provides new interpretations relating to the Heptastadion's construction. The Heptastadion does not appear any longer as a simple communication axis between the island of Pharos, and it is suggested that the objectives of the ancient society, which transformed an open environment into an exploitable and semi-closed context, were twofold: on the one hand, to reduce the influence of currents and agitation of the water-body, and on the other hand, to limit the risk of rapid infilling of the harbour. The origin of the sediments found in the western harbour is mixed, local or Nile derivation, and confirmed by recent authors (Stanley and Hamsa, 1992; Stanley and Wingerath, 1996; Goiran *et al.*, 2003). But in terms of sediment transit, our modelling experiment highlights the major role of the Heptastadion as a structure locally liable to stop the infilling process of the eastern harbour with the prevailing sand-transit flowing from the western harbour. It is probable that the barrier role of the Heptastadion, generally considered as a protection of the eastern harbour against currents only, may have been overestimated in some publications (Bernand, 1966; Goddio *et al.*, 1998), but, conversely, the role of this structure as a protection against sediment-infilling has been generally missed.

Moreover, the persistence in the eastern harbour of a low, but efficient, re-suspension dynamic relating to the finest fractions (silts and clays), locally sustaining a high level of turbidity, allows us to suggest that this autochthonous stock of fine particles can be partly exported offshore through the Silsiley pass (section 5), but partly deposited in the peripheral areas of the harbour featured by weaker currents. In such a hydrodynamic context featuring the eastern harbour in the presence of the Heptastadion, it is possible better to understand the importance and role of the ancient peripheral harbour structures, well described by Goddio *et al.* (1998). Indeed, ancient societies modified and partitioned the rim of the eastern harbour into multiple secondary basins to avoid the risks of sediment-infilling of their installations. We can consider that societies, having to maintain bottoms deep enough for navigation in the eastern harbour of Alexandria, engaged in well-developed protection of the environment by artificialising the coastline in much the same way as modern marinas. At the end of the 1st century BC, Strabo gives some indication of the draught at the bow of ships in this Alexandrian harbour environment: 'As for the Great harbour, in addition to its being beautifully enclosed both by the embankment and by the nature, it is not only so deep close to the shore that the largest ship can be moored at the steps, but also is cut up into several harbours' (Strabo, in Jones, 1959: 27).

Finally, our results allow us to suggest that ancient societies might have managed the environment of the eastern harbour of Alexandria in following a twofold problematic. Firstly, a problematics of navigation: the construction of the

Heptastadion was in part intended to prevent the eastern harbour from inputs of coarse sediment (sand-particles) deriving from the sandy zones of erosion located in the western harbour, in order to maintain a bathymetry favourable to navigation throughout the eastern harbour. Secondly, a problematics of landing: the peripheral structures developed all around the eastern harbour were intended to prevent the landing areas from infilling with fine sediment (silt and clay particles) induced by the local re-suspension processes. More generally, it is possible to presume that the existence of these local erosion zones, and inversely of infill zones, had been frequently noticed by the engineers in antiquity, as a result of their observations of natural banks in Alexandria and widely elsewhere.

Acknowledgements

Research funding and logistical support were provided by the Centre d'Etudes Alexandrines (CEA), UMS-CNRS 1812. We wish to thank Jean-Yves Empereur, director of the CEA in Egypt. This contribution has been also developed with the aid of a Lavoisier franco-egyptian fellowship (for J. P. Goiran) from the French Ministry of the Foreign Office, and with the aid of ANR-JC Scientific Program. Thanks also to MSH network: réseau des Sciences de l'Homme (M. F. Boussac); to Dr Christophe Morhange for constructive criticism of the manuscript; to the Supreme Council of Archaeology of Egypt and the Department of Islamic Antiquities in Alexandria; and to Mohamed Mustafa El Maguib for assistance in the fieldwork.

References

Bernand, A., 1966, *Alexandrie la grande*. Paris.

Coastal Engineering Research Center (CERC), 1975, *Shore Protection Manual*, vol. I. US Army Corps of Engineers, Washington, DC.

El Falaki, M., 1872, *Mémoires sur l'antique Alexandrie*. Copenhagen.

Empereur, J. Y., 1998, *Alexandrie Redécouverte*. Paris.

Etienne, R., Muller, C., and Prost, F., 2000, *Archéologie Historique de la Grèce antique*. Paris.

Frihy, O. E., Dewidar, K. M., and El Raey, M. M., 1996, Evaluation Of Coastal Problems At Alexandria, Egypt, *Ocean and Coastal Management* **30**.2–3, 281–95.

Garvie, A. F., 1994, *Homer, Odyssey*. Cambridge.

Goddio, F., Bernand, A., Bernand, E., Darwish, I., Kiss, Z., and Yoyote, J., 1998, *Alexandrie, les Quartiers Royaux Submergés.* London.

Goiran, J. P., Bourcier, M., and Morhange, C., 2003, Histoire du Colmatage d'un Bassin Portuaire Antique a Alexandrie: L'apport de la sédimentologie et de la Biologie Marine, *Puertos Antiguos: Ciudad, Desarrollo e Infrastructuras. IV Jornadas De Arqueologia Subacuatica*, 319–24. Univ. de Valencia, Facultat de Geografia i Historia.

Hesse, A., Andrieux, P., Atya, M., Benech, C., Camerlynck, C., Debas, M., Fechant, C., Jolivet, A., Kuntz, C., Mechler, P., Panissod, C., Pastor, L., Tabbagh, A., and Tabbagh, J., 2002, L'Heptastadium d'Alexandrie (Egypte), in J. Y. Empereur (ed.), *Alexandrina 2* (*Etudes Alexandrines 6, IFAO 2002*), 191–279.

Jones, H. L., 1959, *The Geography Of Strabo*, Eng. transl. Vol. VIII, **17**.I.6, 27. Cambridge, MA.

Lotfy, M. F. and Badr, A. A., 1999, Long-Term Relief Deformation and Sediment Characteristics of Alexandria Eastern Harbour, Egypt, *Journal of Coastal Research* **15**.1, 266–71.

Millet, B., 1989, Modélisation Hydrodynamique du Bassin de Thau. Validation Ecologique d'un Modèle Numérique de Circulation, *Oceanologica Acta* **12**.1, 37–46.

Millet, B., Blanc, F., and Morhange, C., 2000, Modélisation Numérique de la Circulation des Eaux dans le Vieux-Port de Marseille Vers 600 Ans Avant J-C., *Méditerranée* **94**.1–2, 61–4.

SHOM, 1990, *Abords d'Alexandrie*, Service Hydrographique et Océanographique de la Marine, Carte No. 5923 (1/100.000).

Smyth, W. H., Stater and Elson, 1833, Plan of the City, Harbours and Environs of Alexandria (1/30.000). Hydrographical Office of the Admiralty, London, in Jondet, G. (ed.), *Atlas Historique de la Ville et des Ports d'Alexandrie*, vol. 2, 1921. Cairo.

Soulsby, R. L., 1997, *Dynamics of Marine Sands*. London.

Soulsby, R. L. and Whitehouse, R. J., 1997, Threshold of Sediment Motion in Coastal Environments, *Proc. Pacific Coasts and Ports '97 Conf.*, Christchurch, **1**, 149–54. Canterbury, NZ.

Stanley, D. J. and Hamsa, H., 1992, Terrigenous-Carbonate Sediment Interface (Late Quaternary) along the Northwestern Margin of the Nile Delta, *Journal of Coastal Research* **8**.2, 153–71.

Stanley, D. J. and Wingerath, J. G., 1996, Clay Mineral Distributions to Interpret Nile Cell Provenance and Dispersal: I. Lower River Nile to Delta Sector, *Journal of Coastal Research* **12**.4, 907–10.

UKHO, 1989, Port of Alexandria, UK Hydrographic Office, Chart No. 3554 (1/12.500).

Yoyotte, J., Charvet, P., and Gompertz, S., 1997, *Strabon: le Voyage en Egypte*. Paris.

